Article

Temperature-Induced Switching of the Mechanism for Intramolecular Energy Transfer in a 2,2‘:6‘,2‘ ‘-Terpyridine-Based Ru(II)–Os(II) Trinuclear Array

Andrew C. Benniston, Anthony Harriman, Peiyi Li, and Craig A. Sams

J. Am. Chem. Soc., **2005**, 127 (8), 2553-2564• DOI: 10.1021/ja044097r • Publication Date (Web): 04 February 2005

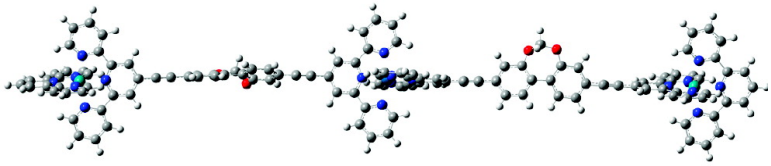

More About This Article

J|A|C|S
ARTICLES
Published on Web 02/04/2005

Temperature-Induced Switching of the Mechanism for Intramolecular Energy Transfer in a 2,2′:6′,2″-Terpyridine-Based Ru(II)−Os(II) Trinuclear Array

Andrew C. Benniston,* Anthony Harriman,* Peiyi Li, and Craig A. Sams

Contribution from the Molecular Photonics Laboratory, School of Natural Sciences−Chemistry, University of Newcastle, Newcastle upon Tyne, NE1 7RU, U.K.

Received September 28, 2004; E-mail: anthony.harriman@ncl.ac.uk

Abstract: The synthesis and photophysical properties of a linear 2,2′:6′,2″-terpyridine-based trinuclear Ru(II)−Os(II) nanometer-sized array are described. This array comprises two bis(2,2′:6′,2″-terpyridine) ruthenium(II) terminals connected via alkoxy-strapped 4,4′-diethynylated biphenylene units to a central bis(2,2′:6′,2″-terpyridine) osmium(II) core. The mixed-metal linear array was prepared using the "synthesis at metal" approach, and the Ru(II)−Ru(II) separation is ca. 50 Å. Energy transfer occurs with high efficiency from the Ru(II) units to the Os(II) center at all temperatures. Förster-type energy transfer prevails in a glassy matrix at very low temperature, but this is augmented by Dexter-type electron exchange at higher temperatures. This latter process, which is weakly activated, involves long-range superexchange interactions between the metal centers. In fluid solution, a strongly activated process provides for fast energy transfer. Here, a charge-transfer (CT) state localized on the bridge is populated as an intermediate species. The CT triplet does not undergo direct charge recombination to form the ground state but transfers energy, possibly via a second CT state, to the Os(II)-based acceptor. The short tethering strap constrains the geometry of the linker, especially in a glassy matrix, such that low-temperature electron exchange occurs across a particular torsion angle of 37°. The probability of triplet energy transfer depends on temperature but always exceeds 75%.

Introduction

Molecular photonics is an emerging area of science concerned with answering the question of how to control and expedite the passage of information quanta along nanoscale molecular wires.[1] To assess the viability of newly synthesized systems, it has proved convenient to study intramolecular electron exchange in mixed-metal $Ru^{II}-Os^{II}$ polypyridyl assemblies since energy migration from Ru^{II} to Os^{II} is thermodynamically favorable.[2−4] The key to efficient through-bond energy transfer lies in the nature of the bridge that connects the two metal centers since this must facilitate strong electronic coupling between the chromophores. Many proposals for the bridging unit have been put forward, including poly(phenylenes),[5] anthracene,[6] naphthalene,[7] thiophene,[8] poly(acetylene),[9] alicyclics,[10] and poly(alkenes).[11] Such studies have been instrumental in improving our understanding of the mechanism of electron exchange and have resulted in the design of prototypes able to transfer

(1) (a) Kubatkin, S.; Danilov, A.; Hjort, M.; Cornil, J.; Bredas, J. L.; Stuhr-Hansen, N.; Hedegard, P.; Bjornholm, T. *Curr. Appl. Phys.* **2004**, *4*, 554−558. (b) Venturi, M.; Balzani, V.; Ballardini, R.; Credi, A.; Gandolfi, M. T. *Int. J. Photoenergy* **2004**, *6*, 1−10. (c) Robertson, N.; McGowan, C. A. *Chem. Soc. Rev.* **2003**, *32*, 96−103.

(2) (a) Constable, E. C.; Handel, R. W.; Housecroft, C. E.; Morales, A. F.; Flamigni, L.; Barigelletti, F. *Dalton Trans.* **2003**, 1220−1222. (b) Akasaka, T.; Otsuki, J.; Araki, K. *Chem.—Eur. J.* **2002**, *8*, 130−136. (c) Pope, S. J. A.; Rice, C. R.; Ward, M. D.; Morales, A. F.; Accorsi, G.; Armaroli, N.; Barigelletti, F. *J. Chem. Soc., Dalton Trans.* **2001**, 2228−2231. (d) Argazzi, R.; Bertolasi, E.; Chiorboli, C.; Bignozzi, C. A.; Itokazu, M. K.; Iha, N. Y. M. *Inorg. Chem.* **2001**, *40*, 6885−6891.

(3) (a) Weldon, F.; Hammarstrom, L.; Mukhtar, E.; Hage, R.; Gunneweg, E.; Haasnoot, J. G.; Reedijk, J.; Browne, W. R.; Guckian, A. L.; Vos, J. G. *Inorg. Chem.* **2004**, *43*, 4471−4481. (b) Akasaka, T.; Inoue, H.; Kuwabara, M.; Mutai, T.; Otsuki, J.; Araki, K. *Dalton Trans.* **2003**, 815−821. (c) Maubert, B.; McClenaghan, N. D.; Indelli, M. T.; Campagna, S. *J. Phys. Chem. A* **2003**, *107*, 447−455. (d) Borje, A.; Kothe, O.; Juris, A. *J. Chem. Soc., Dalton Trans.* **2002**, 843−848. (e) Bilakhiya, A. K.; Tyagi, B.; Paul, P.; Natarajan, P. *Inorg. Chem.* **2002**, *41*, 3830−3842. (f) Hossain, M. D.; Haga, M.; Gholamkhass, B.; Nozaki, K.; Tsuchima, M.; Ikeda, N.; Ohno, T. *Collect. Czech. Chem. Commun.* **2001**, *66*, 307−337.

(4) (a) Serroni, S.; Campagna, S.; Puntoriero, F.; Loiseau, F.; Ricevuto, V.; Passalacqua, R.; Galletta, M. *C. R. Chimie* **2003**, *6*, 883−893. (b) Fleming, C. N.; Dupray, L. M.; Papanikolas, J. M.; Meyer, T. J. *J. Phys. Chem. A* **2002**, *106*, 2328−2334. (c) Baudin, H. B.; Davidsson, J.; Serroni, S.; Juris, A.; Balzani, V.; Campagna, S.; Hammarstrom, L. *J. Phys. Chem. A* **2002**, *106*, 4312−4319. (d) Fleming, C. N.; Maxwell, K. A.; DeSimone, J. M.; Meyer, T. J.; Papanikolas, J. M. *J. Am. Chem. Soc.* **2001**, *123*, 10336−10347. (e) Sommovigo, M.; Denti, G.; Serroni, S.; Campagna, S.; Mingazzini, C.; Mariotti, C.; Juris, A. *Inorg. Chem.* **2001**, *40*, 3318−3323.

(5) (a) Schlicke, B.; Belser, P.; De Cola, L.; Sabbioni, E.; Balzani, V. *J. Am. Chem. Soc.* **1999**, *121*, 4207−4214. (b) Beley, M.; Chodorowski-Kimmes, S.; Collin, J.-P.; Lainé, P.; Launay, J.-P.; Sauvage, J.-P. *Angew. Chem., Int. Ed. Engl.* **1994**, *33*, 1775−1778. (c) Barigelletti, F.; Flamigni, L.; Balzani, V.; Collin, J.-P.; Sauvage, J.-P.; Sour, A.; Constable, E. C.; Cargill Thompson, A. M. W. *J. Am. Chem. Soc.* **1994**, *116*, 7692−7699.

(6) (a) El-ghayoury, A.; Harriman, A.; Ziessel, R. *J. Phys. Chem. A* **2000**, *104*, 7906−7915. (b) Belser, P.; Dux, R.; Baak, M.; De Cola, L.; Balzani, V. *Angew. Chem., Int. Ed. Engl.* **1995**, *34*, 595−598.

(7) El-ghayoury, A.; Harriman, A.; Khatyr, A.; Ziessel, R. *J. Phys. Chem. A* **2000**, *104*, 1512−1523.

(8) (a) Encinas, S.; Flamigni, L.; Barigelletti, F.; Constable, E. C.; Housecroft, C. E.; Shofield, E. R.; Figgemeier, E.; Fenske, D.; Neuburger, M.; Vos, J. G.; Zehnder, M. *Chem.—Eur. J.* **2002**, *8*, 137−150. (b) Ringenbach, C.; De Nicola, A.; Ziessel, R. *J. Org. Chem.* **2003**, *68*, 4708−4719. (d) Harriman, A.; Mayeux, A.; De Nicola, A.; Ziessel, R. *Chem. Phys. Phys. Chem.* **2002**, *4*, 2229−2235.

(9) (a) Harriman, A.; Khatyr, A.; Ziessel, R.; Benniston, A. C. *Angew. Chem., Int. Ed.* **2000**, *39*, 4287−4291. (b) Harriman, A.; Romero, F. M.; Ziessel, R.; Benniston, A. C. *J. Phys. Chem. A* **1999**, *103*, 5399−5408. (c) Grosshenny, V.; Harriman, A.; Hissler, M.; Ziessel, R. *J. Chem. Soc., Faraday Trans.* **1996**, *92*, 2223−2238.

excitation energy over relatively long distances.[12] In seeking to control the rate of through-bond electron transfer, it seems appropriate to develop the capacity to fine-tune the electronic properties of the bridge.[13] One way in which this level of control might be realized is to insert a ratchet into the bridge that can be adjusted to predetermined positions, each of which favors a particular rate of energy transfer along the molecular axis. A ratchet of this type might be constructed, for example, by tethering the 2,2′-positions of a bridging biphenylene unit with a strap of variable length in such a way that each strap imposes a narrow range of torsion angles.[14] There is evidence to the effect that the degree of electronic coupling along a short molecular wire depends on the torsion angle.[15]

Before embarking on the synthesis of a series of such elaborate supermolecules, it seems prudent to ensure that intramolecular energy transfer does takes place through a biphenylene unit since the basic structure places the terminal metal centers some 25 Å apart.[16] To this effect, we have synthesized a linear, trinuclear array, **RBOBR**, equipped with the necessary functionality to test the feasibility of this project. The selected system possesses two donors attached to a central acceptor via two identical bridges, but at any given time, only one arm of the system is operating. Thus, the ruthenium(II) bis-(2,2′:6′,2″-terpyridine)-based (Ru-terpy) terminals are intended to act as energy donors for the central osmium(II) bis(2,2′:6′,2″-terpyridine)-based (Os-terpy) core. The acceptor complex is known to emit in fluid solution at room temperature,[17] thereby facilitating the study of intramolecular excitation energy redistribution. A dialkoxy strap attached at the 2,2′-positions of the biphenylene unit is intended to constrain the geometry of the bridge.[14] Biphenyl exists in solution with a torsion angle of 44°, but on reduction to the π-radical anion, the two phenylene rings can adopt a coplanar geometry.[18] The short constraining strap favors a torsion angle of 37° for the ground state, although atropisomerism is introduced and prevents adoption of a coplanar structure. Within reason, the torsion angle can be controlled by the length of the strap. Preparation of the supermolecule uses the "synthesis at metal" approach,[19] which is gaining wide usage since metal centers are introduced early in the synthetic procedure and enhance solubility. The main objective of this study is to establish the mechanism for intramolecular triplet energy transfer and to enquire if the rate might be modulated by changes in torsion angle. During the course of this investigation it became clear that the mechanism depends on the temperature and/or environment.

Experimental Section

All raw materials were purchased from Aldrich Chemicals Co. and were used as received. Solvents were dried by standard literature methods before being distilled and stored under nitrogen over 4 Å molecular sieves.[20] The starting materials, Ru-terpy[21] (terpy = 2,2′:6′,2″-terpyridine) and 4′-trimethylsilylethynyl-[2,2′:6′,2″]-terpy **1**,[22] were prepared by literature methods. The synthetic procedure used to isolate the target compound is given in Scheme 1. ^{1}H and ^{13}C NMR spectra were recorded with JEOL Lambda 500 MHz or Bruker AVANCE 300 MHz spectrometers. Routine mass spectra and elemental analyses were obtained using in-house facilities. Absorption spectra were recorded with a Hitachi U3310 spectrophotometer, while corrected emission spectra were recorded with a Yvon-Jobin Fluorolog tau-3 spectrophotometer. All luminescence measurements were made using optically dilute solutions and were corrected for spectral imperfections of the instrument by reference to a standard lamp. Luminescence quantum yields were determined relative to osmium(II) bis(2,2′:6′,2″-terpyridine) in acetonitrile solution.[23] Time-resolved luminescence measurements were made after excitation of the sample with a 4 ns laser pulse delivered at 480 nm and with a repetition rate of 1 kHz. Luminescence was isolated from scattered laser light with a high radiance monochromator and detected with a Ge photocell operated at −10 °C. Approximately, 20 000 individual records were collected and averaged prior to storage. Data analysis was made after deconvolution of the instrument response function. Temperature-dependent studies were made with an Oxford Instruments Optistat DN cryostat.

Transient absorption studies were made by conventional methods after excitation with a 5 ns laser pulse delivered at either 532 or 480 nm from a Q-switched Nd:YAG laser. In the latter case, the laser beam was focused through a 1 m cell filled with deuterium, and the required excitation line was isolated with a prism coupled to a narrow band-pass filter. The monitoring beam was provided with a pulsed Xe arc lamp and was detected with a fast response PMT. Data analysis was made at a fixed wavelength by signal-averaging methods. The sample was deoxygenated by purging with N_2. Other studies used a frequency-doubled, mode-locked Nd:YAG laser as excitation source. Here, the laser pulse (fwhm = 25 ps) was Raman shifted to 480 nm. Residual laser light was used to generate a white light continuum for use as the monitoring beam. The two beams were passed almost collinearly through the sample cell, and the monitoring beam was dispersed with a Spex spectrograph and detected with a Princeton dual-diode array spectrometer. Approximately 200 individual laser shots were averaged at each delay time. Again, the sample was deoxygenated by purging with N_2. Temperature-dependent studies were made with an Oxford Instruments Optistat DN cryostat.

Reduction potentials were measured by cyclic voltammetry using an HCH electrochemical analyzer. The working electrode was a polished glassy carbon disk, while the counter electrode was a Pt wire. The Ag/

(10) (a) Kelso, L. S.; Smith, T. A.; Schultz, A. C.; Junk, P. C.; Warrener, R. N.; Ghiggino, K. P.; Keene, R. R. *J. Chem. Soc., Dalton Trans.* **2000**, 2599−2606. (b) Juris, A.; Prodi, L.; Harriman, A.; Ziessel, R.; Hissler, M.; Elghayoury, A.; Wu, F.; Riesgo, E. C.; Thummel, R. *Inorg. Chem*. **2000**, *39*, 3590−3598. (c) Hammarstrom, L.; Barigelletti, F.; Flamigni, L.; Armaroli, N.; Sour, A.; Collin, J.-P.; Sauvage, J.-P. *J. Am. Chem. Soc.* **1996**, *118*, 11972−11973.
(11) (a) Tung, C. H.; Zhang, L. P.; Li, Y.; Cao, H.; Tanimoto, Y. *J. Am. Chem. Soc*. **1997**, *119*, 5348−5354. (b) Benniston, A. C.; Goulle, V.; Harriman, A.; Lehn, J.-M. *J. Phys. Chem.* **1994**, *98*, 7798−7804.
(12) (a) Hofmeier, H.; Schubert, U. S. *Chem. Soc. Rev*. **2004**, *33*, 373−399. (b) Baranoff, E.; Collin, J.-P.; Flamigni, L.; Sauvage, J.-P. *Chem. Soc. Rev*. **2004**, *33*, 147−155. (c) Barigelletti, F.; Flamigni, L. *Chem. Soc. Rev*. **2000**, *29*, 1−12. (d) Harriman, A.; Ziessel, R. *Chem. Commum*. **1996**, 1707−1716.
(13) (a) Peskin, U.; Abu-Hilu, M.; Spieser, S. *Opt. Mater*. **2003**, *24*, 23−29. (b) Kyrychenko, A.; Albinsson, B. *Chem. Phys. Lett*. **2002**, *366*, 291−299. (c) Hurley, D. J.; Tor, Y. *J. Am. Chem. Soc*. **2002**, *124*, 13231−13241.
(14) (a) Benniston, A. C.; Li, P.; Sams, C. *Tetrahedron Lett*. **2003**, *44*, 3947−3950. (b) Benniston, A. C.; Harriman, A.; Li, P.; Sams, C. *Tetrahedron Lett*. **2003**, *44*, 4167−4169. (c) Maus, M.; Rettig, W. *Phys. Chem. Chem. Phys.* **2001**, *3*, 5430−5437.
(15) (a) Toutounji, M. M.; Ratner, M. A. *J. Phys. Chem. A* **2000**, *104*, 8566−8569. (b) Paulson, B. P.; Curtiss, L. A.; Bal, B.; Closs, G. L.; Miller, J. R. *J. Am. Chem. Soc*. **1996**, *118*, 378−387.
(16) Although triplet−triplet energy transfer can occur over relatively long distances (e.g., 50 Å), it is necessary that this process competes effectively with nonradiative decay of the excited state. The triplet lifetime of the Ru-terpy reference compound is only 25 ns, and it is well established that the rate of electron exchange decreases exponentially with increasing separation.
(17) Sauvage, J.-P.; Collin, J.-P.; Chambron, J.-C.; Guillerez, S.; Coudret, C.; Balzani, V.; Barigelletti, F.; De Cola, L.; Flamigni, L. *Chem. Rev*. **1994**, *94*, 993−1019.
(18) (a) Cacelli, I.; Prampolini, G. *J. Phys. Chem. A* **2003**, *107*, 8665−8670. (b) Grein, F. *J. Phys. Chem. A* **2002**, *106*, 3823−3827.
(19) Fraysse, S.; Coudret, C.; Launay, J. P. *J. Am. Chem. Soc.* **2003**, *125*, 5880−5888.
(20) Perrin, D. D.; Armarego, W. L. F. *Purification of Laboratory Chemicals*, 3rd edition; Permagon Press Ltd.: Oxford, 1988.
(21) Sullivan, B. P.; Calvert, J. M.; Meyer, T. J. *Inorg. Chem.* **1980**, *19*, 1404−1407.
(22) Potts, K. T.; Konwar, D. *J. Org. Chem.* **1991**, *56*, 4815−4816.
(23) Demas, J. N.; Crosby, G. A. *J. Am. Chem. Soc.* **1971**, *93*, 2841−2847.

Scheme 1. Outline of the Procedure Used To Prepare the Target Complex RBOBR

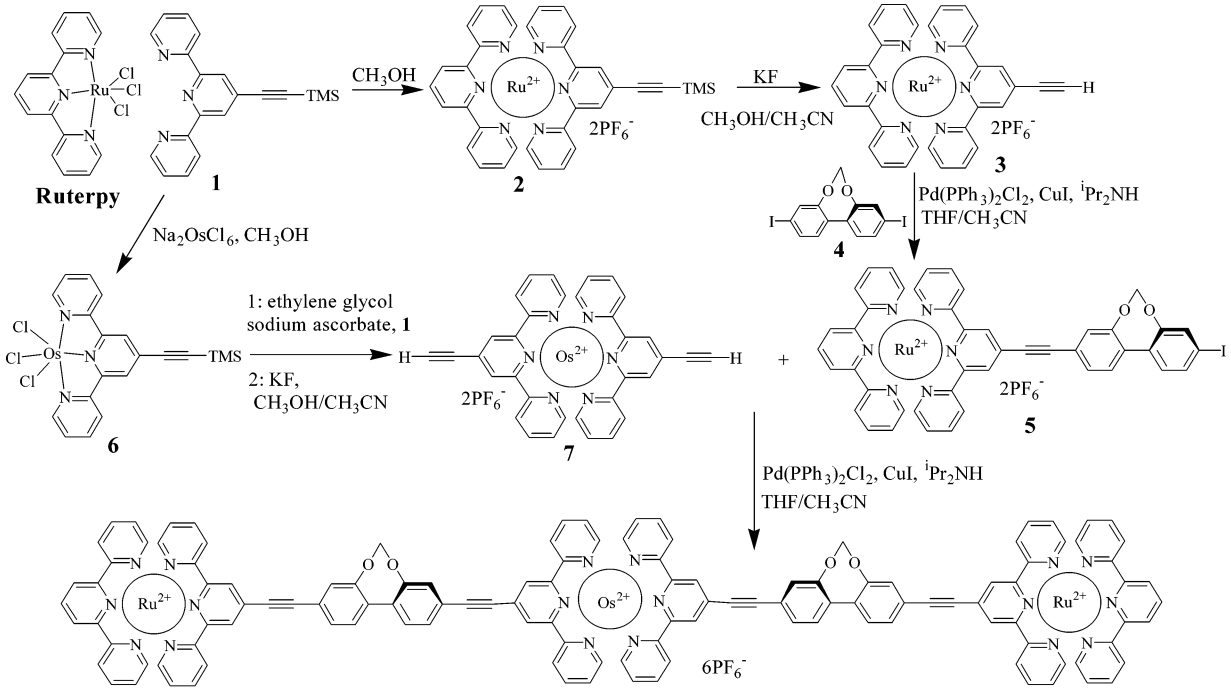

RBOBR

AgCl reference electrode was separated from the electrolysis cell by a glass frit. The solution contained the solute (ca. 1.2 mM) and tetra-*N*-butylammonium hexafluorophosphate (0.2 M) as background electrolyte and was purged with N_2 prior to electrolysis. Ferrocene was used as internal standard.

Molecular dynamics simulations were performed using Insight-II running on a Silicon Graphics Iris 02+ workstation. The structure of the compound was drawn using the Builder module within the package, and partial charges were assigned using the esff force-field. There were no cutoffs for nonbonding interactions. The energy of the structure in vacuo was minimized using the Discover_3 module and the Newton−Raphson algorithm, until the maximum derivative was less than 0.001 kcal/Å. This structure was used as the starting point for the molecular dynamics simulations (MDS). The MDS studies consisted of an initial 10 000 fs of equilibration using the velocity scaling method, followed by 20 000 fs of dynamics carried out under the Anderson method. During this latter stage, the temperature averaged 299 K with a standard deviation of ±3.2 K, and data points were collected every 10 fs.

Subsequent MDS runs were performed in a solvent bath with 1286 water molecules and a total of six PF_6^- counterions. Due to the large number of atoms involved in these calculations, energy-minimized structures were calculated using the conjugate gradient method and with a cutoff of 15 Å for nonbonding interactions. The MDS studies were performed as described above. These simulations show that considering explicit solvent molecules tends to dampen the torsional fluctuations.

[Ru(terpy)(4′-trimethylsilylethynyl-terpy)](PF$_6$)$_2$] (2). 4′-Trimethylsilylethynyl-terpy **1** (630 mg, 1.91 mmol) and *N*-ethylmorpholine (0.35 mL) were added to a suspension of [Ru(terpy)Cl_3] (800 mg, 1.82 mmol) in CH_3OH (180 mL). The mixture was refluxed under N_2 for 4 h, cooled to room temperature, and filtered. The solvent volume was reduced to ca. 50 mL, and an aqueous KPF_6 (3.0 g, 0.0163 mol) solution was added to afford a dark red solid which was filtered and washed with H_2O and diethyl ether before being dried in vacuo. Yield: 1.44 g (83%). This material was used in subsequent desilylation reactions without further purification.

[Ru(terpy)(4′-ethynyl-terpy)](PF$_6$)$_2$] (3). To the dark red solution of crude [Ru(terpy)(4′-trimethylsilylethynyl-terpy)](PF$_6$)$_2$] (1.00 g, 1.04 mmol) in CH_3CN (80 mL) was added KF (1.21 g, 20.8 mmol) dissolved in CH_3OH (40 mL). The mixture was stirred overnight at room temperature before removal of the solvent on a rotary evaporator. The crude residue was redissolved in CH_3CN and filtered to remove KF impurities. The filtrate was reduced in volume and subjected to silica gel column chromatography using CH_3CN:H_2O:saturated KNO_3 (85:14:1) as eluent. The combined fractions of the desired product were reduced in volume, and an aqueous KPF_6 solution was added to precipitate a bright red solid, which was filtered, washed with H_2O and diethyl ether, and dried in vacuo. Yield: 0.41 g (44%, based on the crude starting material). The ^{1}H NMR spectrum of the product was identical to that reported in the literature but was prepared by a different route.[24]

9-Diiodo-5,7-dioxadibenzo[a,c]cycloheptene (4). To a solution of 4,4′-diiodo-2,2′-biphenol (0.8 g, 1.83 mmol) in dry DMF (40 mL) was added K_2CO_3 (0.65 g, 4.70 mmol). The mixture was stirred under N_2 at 90 °C for 1.5 h, followed by the slow addition of CH_2I_2 (0.16 mL, 1.97 mmol) in dry DMF (20 mL). The mixture was heated under N_2 at 90 °C for a further 24 h before removal of the DMF on a rotary evaporator. The residue was extracted into ethyl acetate, washed with H_2O, separated, and dried over $MgSO_4$. Removal of the organic solvent afforded a crude product which was purified by medium-pressure silica gel column chromatography using petrol:ethyl acetate (9:1) as the eluent. Yield: 0.49 g (60%). ^{1}H NMR (δ, 300 MHz, $CDCl_3$): 5.55 (s, 2H, H of methylene), 7.35 (d, J = 8.2 Hz, 2H, Ph−H^6), 7.52−7.56 (d and dd, J = 8.2 Hz, J_{av} = 1.7 Hz, 4H, Ph−H^{3,5}). EI-MS (m/z): 450 (calcd M_r = 449.86 for $C_{13}H_8O_2I_2$).

[Ru(terpy)(4′-(9-iodo-5,7-dioxadibenzo[a,c]cyclohepten-3-ylethynyl)) [2,2′:6′,2″]terpy)](PF$_6$)$_2$ (5). Under a N_2 atmosphere, 3,9-diiodo-5,7-dioxadibenzo[a,c]cycloheptene (200 mg, 0.444 mmol), Pd(PPh_3)$_2$-Cl_2 (31 mg, 0.044 mmol), and CuI (17 mg, 0.089 mmol) were dissolved in an ^{i}Pr_2NH (20 mL)/THF (60 mL)/CH_3CN (20 mL) solvent mixture. The yellow solution was brought to reflux, and [Ru(terpy)(4′-ethynyl-terpy)](PF$_6$)$_2$] (392 mg, 0.444 mmol) in CH_3CN (50 mL) was added slowly via a syringe pump. The solution was maintained at reflux during the addition over 2 days. After the mixture was cooled to room

(24) Uyeda, H. T.; Zhao, Y.; Wostyn, K.; Asselberghs, I.; Clays, K.; Persoons, A.; Therien, M. J. *J. Am. Chem. Soc.* **2002**, *124*, 13806−13813.

temperature, the solvents were removed and the residue was redissolved in CH_3NO_2 and filtered to remove impurities. The CH_3NO_2 filtrate was washed with dilute HCl, Na_2CO_3 (aq.), and water, separated, and dried over $MgSO_4$. The crude product was purified by silica column chromatography using CH_3CN:H_2O:saturated KNO_3 (90:14:1) as the eluent. The combined fractions of the desired product ($R_f = 0.64$) were reduced in volume, and an aqueous KPF_6 solution was added to precipitate a red solid which was filtered, washed with H_2O and diethyl ether, and dried in vacuo. Yield: 179 mg (46%, based on iodo starting material). ^{1}H NMR (δ, 300 MHz, CD_3CN): 8.70 (s, 2H, terpy-H$^{3',5'}$), 8.58 (d, 2H, $J = 8.1$ Hz, terpy-H$^{3',5'}$), 8.32 (m, 4H, terpy-H$^{6,6''}$), 8.26 (t, 1H, $J = 8.1$ Hz, terpy-H$^{4'}$), 7.76 (m, 5H, terpy-H$^{5,5''}$ and Ph−H), 7.37−7.52 (m, 5H, Ph−H), 7.20 (m, 4H, terpy-H$^{3,3''}$), 7.00 (m, 4H, terpy-H$^{4,4''}$), 5.49 (s, 2H, $-CH_2-$). ESI-MS (*m*/*z*): 1059.1 (calcd 1059.0 for $[M - PF_6]^+$), 913.1 (calcd 913.0 for $[M - PF_6 - HPF_6]^+$), 457.0 (calcd 457.0 for $[M - PF_6]^{2+}$). Anal. Calcd for $RuC_{45}H_{29}N_6O_2I \cdot P_2F_{12}$: C, 44.90; H, 2.43; N, 6.98. Found: C, 45.34; H, 2.45; N, 7.09. A minor product (140 mg) was also isolated and identified as the dinuclear complex, [(terpy)Ru(5,7-dioxadibenzo[a,c]cyclohepten-3,9-yl-di(ethynyl[2,2′:6′,2″]-terpyridine))Ru(terpy)]$(PF_6)_4$. This unexpected formation of the dinuclear complex reduced the yield of the desired mononuclear product.

[Os(4′-trimethylsilylethynyl-terpy)Cl$_3$] (6). To a solution of Na_2OsCl_6 (200 mg, 0.412 mmol) in CH_3OH (30 mL) was added 4′-trimethylsilylethynyl-terpy **1** (140 mg, 0.425 mmol). The mixture was refluxed under N_2 for 20 h, during which time the color turned from green to deep red and was accompanied by formation of a dark precipitate. The reaction mixture was cooled to room temperature and refrigerated overnight. The resultant dark brown precipitate was filtered, washed with CH_3OH and diethyl ether, and dried in vacuo. Yield: 200 mg (78%).

[Os(4′-trimethylsilylethynyl-terpy)$_2$](PF$_6$)$_2$ (7a). To a suspension of Os(4′-trimethylsilylethynyl-terpy)Cl_3 (190 mg, 0.303 mmol) in ethylene diglycol (20 mL) were added 4′-trimethylsilylethynyl-terpy **1** (100 mg, 0.303 mmol) and sodium ascorbate (80 mg, 0.404 mmol). The mixture was heated under N_2 at 110 °C for 20 h. After being cooled to room temperature, the reaction mixture was diluted with H_2O (150 mL) and treated with an aqueous KPF_6 (1.5 g, 8.15 mmol) solution. Refrigeration overnight resulted in precipitation of a solid which was collected by filtration, washed with H_2O and diethyl ether, and purified by silica gel column chromatography using CH_3CN:H_2O:saturated KNO_3 (90:10:1) as the eluent. The combined fractions of the desired product ($R_f = 0.55$) were reduced in volume, and a KPF_6 aqueous solution was added to precipitate a black solid which was filtered, washed with H_2O and diethyl ether, and dried in vacuo. Yield: 160 mg (46%). ^{1}H NMR (δ, 300 MHz, CD_3CN): 8.59 (s, 4H, terpy-H$^{3',5'}$), 8.29 (d, 4H, $J = 8.2$ Hz, terpy-H$^{6,6''}$), 7.61 (m, 4H, terpy-H$^{5,5''}$), 7.05 (d, 4H, $J = 5.6$ Hz, terpy-H$^{3,3''}$), 6.92 (m, 4H, terpy-H$^{4,4''}$), 0.23 (s, 18H, $-Si(CH_3)_3$).

[Os(4′-ethynyl-terpy)$_2$](PF$_6$)$_2$ (7). To a dark brown solution of [Os(4′-trimethylsilylethynyl-terpy)$_2$]$(PF_6)_2$ (160 mg, 0.14 mmol) in CH_3CN (20 mL) was added KF (160 mg, 2.75 mmol) dissolved in CH_3OH (20 mL). The mixture was stirred overnight at room temperature, cooled, and the solvent removed. The residue was redissolved in CH_3CN and filtered to remove KF impurities. The filtrate was reduced in volume and subjected to silica gel column chromatography using CH_3CN:H_2O:saturated KNO_3 (90:10:1) as eluent. The combined fractions of the desired product ($R_f = 0.56$) were reduced in volume, and an aqueous KPF_6 solution was added to precipitate a black solid which was filtered and washed with H_2O and diethyl ether. The pure product was obtained as violet microcrystals by slow vapor diffusion of diethyl ether into a concentrated CH_3CN solution of the material. Yield: 90 mg (64%). ^{1}H NMR (δ, 300 MHz, CD_3CN): 8.66 (s, 4H, terpy-H$^{3',5'}$), 8.29 (d, 4H, $J = 7.9$ Hz, terpy-H$^{6,6''}$), 7.62 (m, 4H, terpy-H$^{5,5''}$), 7.06 (d, 4H, $J = 5.1$ Hz, terpy-H$^{3,3''}$), 6.93 (m, 4H, terpy-H$^{4,4''}$), 3.76 (s, 2H, $-C\equiv C-H$). ESI-MS (*m*/*z*): 851.2 (calcd 851.1 for $[M - PF_6]^+$), 352.1 and 353.1 (calcd 351.1 and 353.1 for $[M - 2PF_6]^{2+}$). Anal. Calcd for $OsC_{34}H_{22}N_6 \cdot P_2F_{12}$: C, 41.05; H, 2.23; N, 8.45. Found: C, 41.36; H, 2.22; N, 8.25.

Preparation of RBOBR. Under a N_2 atmosphere, [Ru(terpy)(4′-(9-iodo-5,7-dioxadibenzo[a,c]cyclohepten-3-ylethynyl)[2,2′:6′,2″]-terpyridine)]$(PF_6)_2$ (70 mg, 0.058 mmol), [Os(4′-ethynyl-terpy)$_2$]$(PF_6)_2$ (25 mg, 0.025 mmol), $Pd(PPh_3)_2Cl_2$ (7 mg, 0.010 mmol), and CuI (4 mg, 0.021 mmol) were dissolved in a mixture of ^{i}Pr$_2$NH (10 mL)/THF (20 mL)/CH_3CN (30 mL). The mixture was refluxed under N_2 for 20 h, followed by removal of all solvent. The residue was redissolved in CH_3NO_2 and filtered. The CH_3NO_2 filtrate was washed with dilute HCl, Na_2CO_3 (aq.), and H_2O before being dried over $MgSO_4$. The crude product obtained following solvent removal was purified by silica column chromatography using CH_3CN:H_2O:saturated KNO_3 (85:14:1) as eluent. The combined fractions of the desired product ($R_f = 0.48$) were reduced in volume, and an aqueous KPF_6 solution was added to precipitate the required material. The red−brown solid was collected and washed with H_2O and separated by centrifugation. The pure product was obtained by two recrystallizations from CH_3CN/diethyl ether. Yield: 27 mg (24%). ^{1}H NMR (δ, 500 MHz, CD_3CN): 8.77 (s, 4H, terpy-H$^{3',5'}$), 8.74 (s, 4H, terpy-H$^{3',5'}$), 8.60 (d, 4H, $J = 8.1$ Hz, terpy-H$^{3',5'}$), 8.35 (m, 12H, terpy-H$^{6,6''}$), 8.28 (t, 2H, $J = 8.1$ Hz, terpy-H$^{4'}$), 7.88 (dd, 4H, $J = 8.5$ Hz, $J = 2.1$ Hz, Ph−H), 7.79 (m, 8H, terpy-H$^{5,5''}$), 7.69 (m, 4H, terpy-H$^{5,5''}$), 7.55 (m, 4H, Ph−H), 7.44 (d, 2H, $J = 1.8$ Hz, Ph−H), 7.46 (d, 2H, $J = 1.8$ Hz, Ph−H), 7.15−7.24 (m, 12H, terpy-H$^{3,3''}$), 6.99−7.06 (m, 12H, terpy-H$^{4,4''}$), 5.62 (s, 4H, $-CH_2-$). MALDI-MS (matrix, DCTB) (*m*/*z*): 3001.2 (calcd 3001.2 for $[M - PF_6]^+$), 2855.3 (calcd 2856.3 for $[M - 2PF_6]^+$), 1428.2 (calcd 1428.2 for $[M - 2PF_6]^{2+}$), 1188.2 (calcd 1188.1 for fragment [(terpy)-Ru(terpy)−C≡C−(methylene-2,2′-dioxa-bridged biphenyl)−C≡C−(terpy)$(PF_6)]^+$). Anal. Calcd for $C_{124}H_{78}N_{18}O_4P_6F_{36}Ru_2Os \cdot 3H_2O$: C, 46.54; H, 2.65; N, 7.88. Found: C, 46.23; H, 2.54; N, 7.89.

Results and Discussion

Synthesis. Numerous polynuclear $Ru^{II}-Os^{II}$ complexes have been reported over the past decade or so.[12] The metal centers have been connected by organic,[2−4] organometallic,[9d] and supramolecular moieties,[25] and the arrays have been extended from simple linear structures to dendrimers[3g,4a,d,f] and metallopolymers.[4c,e] In many cases, intramolecular triplet energy transfer has been described and used, for example, to probe how the rate constant depends on separation distance,[5b,d,e,9b,e] temperature,[10d] type of spacer group,[5−11] and orientation.[9d] The target supermolecule under study here (Figure 1) has been designed as a prototype for the examination of how the rate of triplet energy transfer depends on the torsion angle of a bridging biphenylene unit. The terminal metal complexes were built around 2,2′:6′,2″-terpyridine ligands so as to avoid problems of chirality, but it is well-known that Ru-terpy is essentially nonluminescent at ambient temperature.[26] Emission is switched on if alkynylene groups are attached to the 4′-position of the terpyridine ligand.[27] Consequently, the connecting unit should comprise a 4,4′-diethynylated biphenylene residue. To introduce a ratchet that can control the torsion angle, without perturbing the electronic level of the bridge, a dialkoxy strap is attached at the 2,2′-positions of the biphenylene unit. This work uses a short strap, but the synthetic procedure can be adapted to produce a range of such complexes with different strap

(25) Odobel, F.; Massiot, D.; Harrison, B. S.; Schanze, K. S. *Langmuir* **2003**, *19*, 30−39.
(26) (a) Amini, A.; Harriman, A.; Mayeux, A. *Phys. Chem. Chem. Phys.* **2004**, *6*, 1157−1164. (b) Winkler, J. R.; Netzel, T. L.; Creutz, C.; Sutin, N. *J. Am. Chem. Soc.* **1987**, *109*, 2381−2392.
(27) Benniston, A. C.; Chapman, G. M.; Harriman, A.; Mehrabi, M.; Sams, C. A. *Inorg. Chem.* **2004**, *43*, 4227−4233.

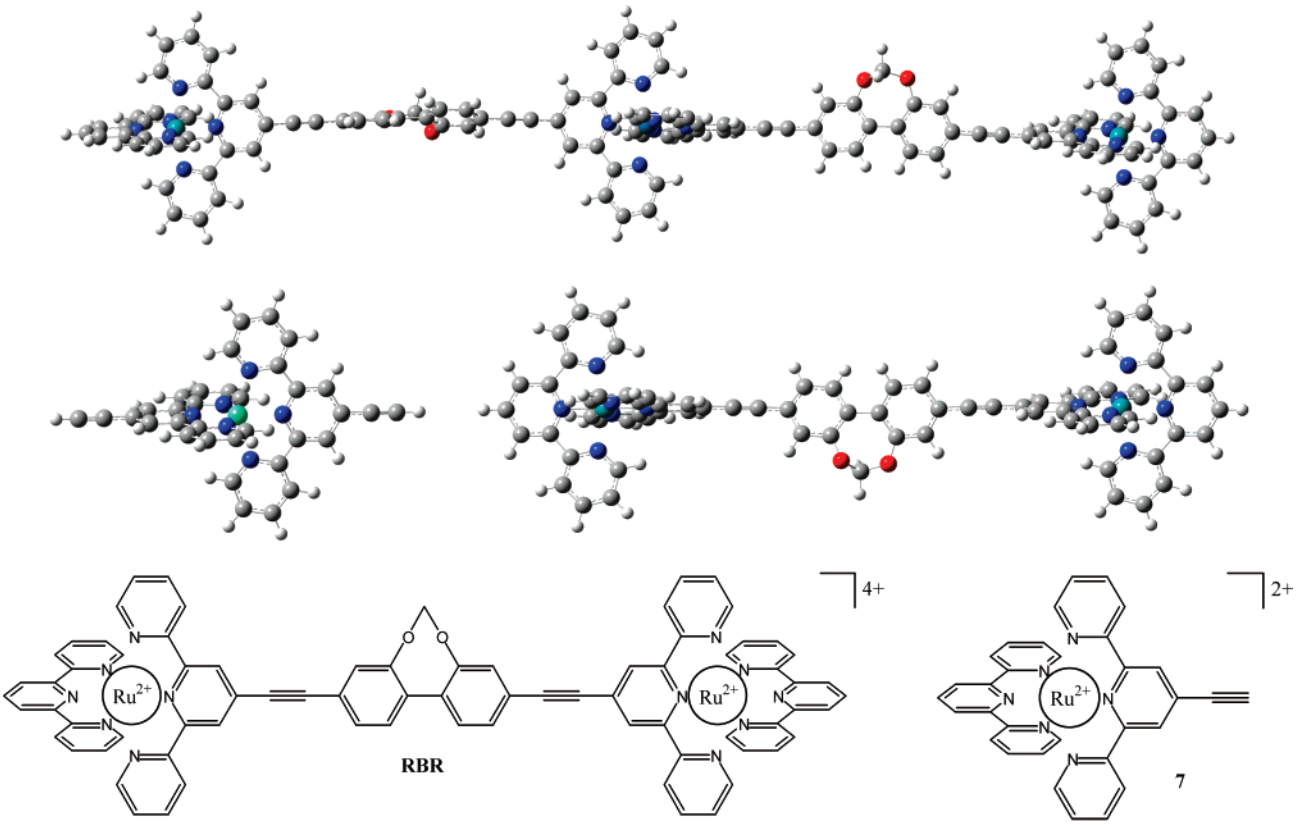

Figure 1. Structural formulas for the target complex, **RBOBR**, and the two reference complexes, **7** and **RBR**.

lengths.[14b] The strap can also be modified to include heteroatoms.[14a] In this latter case, the torsion angle can be further refined by wrapping the strap around selected cations. It should be noted that Ziessel et al.[28] have described a 2,2′-bipyridyl-bridged binuclear complex, but we are unaware of any related systems where the geometry of the central connector can be modulated systematically.

In an earlier communication,[14b] we described the synthesis of appropriate 2,2′:6′,2″-terpyridine-based ligands and their homoleptic ruthenium(II) complexes. Using this method, the metal centers were attached toward the end of the synthesis. However, it was found that mixed-metal complexes could not be prepared this way because of the poor ligand solubility since all attempts to produce a mono-ruthenium(II) 2,2′:6′,2″-terpyridine synthon gave only the bimetallic complex. Hence, outlined in Scheme 1 is the alternative synthetic approach used to prepare **RBOBR**, starting from Ru-terpy and the TMS-protected ligand **1**. This method is superior since the various synthons are soluble in common organic solvents and chromatographic separations are straightforward. Refluxing **1** and Ru-terpy in methanol containing *N*-ethylmorphine as reductant produced complex **2** in a respectable 83% yield. The silyl protecting group of **2** was removed using KF to afford after column chromatography (silica gel:CH_3CN:H_2O:saturated KNO_3, 85:14:1) derivative **3**. Careful cross-coupling of **3** with the methylene-strapped biphenylene derivative **4** afforded the mono-ruthenium(II) complex **5** in 33% yield. The osmium(II) portion of the supermolecule was prepared in a stepwise manner, starting from derivative **1**. Thus, reaction of **1** with sodium hexachloroosmate in methanol produced the mono-terpy synthon **6** in 78% yield. Derivative **7** was prepared in two further steps by reacting **6** with 1 equiv of **1**, followed by deprotection. Using standard cross-coupling conditions, reaction of **7** with **5** produced after column chromatography (silica gel:CH_3CN:H_2O:saturated KNO_3, 85:14:1) the desired complex as a red−brown solid in an unoptimized yield of 24%. Authenticity of the final complex and precursors was made by standard analytical techniques, including ^{1}H NMR spectroscopy, mass spectrometry, and elemental composition.

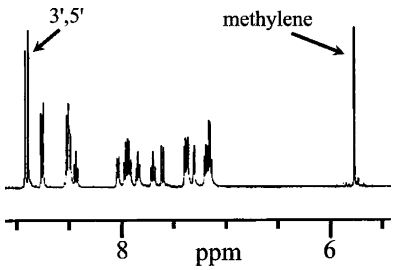

Figure 2. Partial ^{1}H NMR spectrum recorded for **RBOBR** in CD_3CN showing an expanded view of the aromatic region.

The simplicity of the ^{1}H NMR spectrum recorded for **RBOBR** in CD_3CN (Figure 2) clearly supports the supposed high level of symmetry in the complex. The typical aromatic resonances associated with the 2,2′,6′,2″-terpyridine and 4,4′-biphenylene groups are well resolved. Two distinct singlets at δ ~8.7 and 8.4 ppm are readily assigned to the 3′,5′ protons of the ethynylene-substituted 2,2′,6′,2″-terpyridine ligand associated with the Ru^{II} and Os^{II} centers. Moreover, the relatively sharp signal at 5.7 ppm can be assigned to the methylene protons of the bridge. This short bridging unit is expected to restrict the torsion angle around the central biphenylene unit. Close

(28) Hissler, M.; El-ghayoury, A.; Harriman, A.; Ziessel, R. *Angew. Chem., Int. Ed.* **1998**, *37*, 1717−1720.

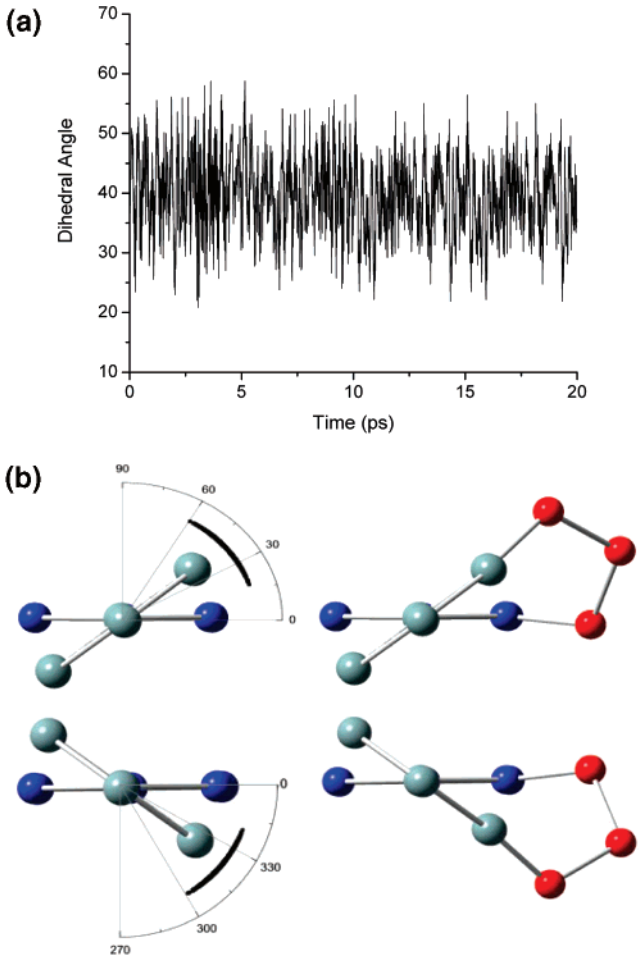

Figure 3. (a) Pictorial representation of the atropisomers formed because of restricted rotation around the biphenylene unit. The scale represents the maximum degree of internal flexibility for the torsion angle as determined by molecular dynamics simulations. (b) Variation of the biphenylene torsion angle during a MDS run.

examination of the structure suggests that **RBOBR** might exist as a mixture of atropisomers due to restricted rotation around the biphenylene central bond. Indeed, molecular dynamics simulations of the bridge portion of **RBOBR** in a solvent bath showed that there is partial twisting of the two phenylene units of the bridge, with the torsion angle between the two rings extending between 54 and 20° (Figure 3).[29] The average torsion angle is 37°, but this idealized structure is likely to persist only at low temperature. The MDS studies indicate that the atropisomers do not interconvert because the strap prevents the biphenylene unit from adopting a coplanar geometry. The appearance of atropisomers is not apparent from the ^{1}H NMR spectra recorded at room temperature. Molecular dynamics studies made with the full molecule show that the outer Ru-terpy units undergo a "wagging" motion with the central osmium moiety behaving as an inertial pivot. It is possible, therefore, that the metalloterminals introduce increased flexibility into the system that permits rotation around the central biphenylene. This would prevent formation of atropisomers. It should also be noted that, since low intensity illumination is used, only one donor is excited at any given time.

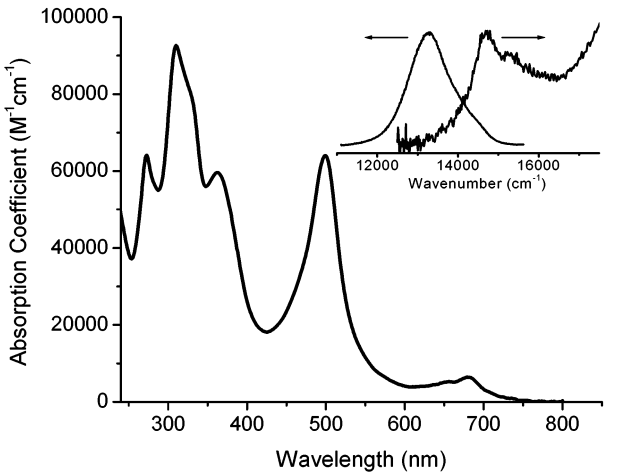

Figure 4. UV−visible absorption and luminescence spectra recorded for **RBOBR** in deoxygenated butyronitrile at room temperature.

Electrochemical Properties. The redox behavior of **RBOBR** was studied in acetonitrile solution (0.2 M tetra-*N*-butylammonium hexafluorophosphate as background electrolyte) using cyclic voltammetry. On oxidative scans, two quasi-reversible waves were evident at $E_1 = +1.05$ V (1e, $\Delta E_p = 80$mV) vs Ag/AgCl and $E_2 = +1.37$ V (2e, $\Delta E_p = 70$mV) vs Ag/AgCl. These peaks correspond to redox processes taking place at the Os^{II} and Ru^{II} centers, respectively. The observed half-wave potentials are in good agreement with related alkynylene-substituted Os^{II} and Ru^{II} terpyridine complexes.[30] There was no indication for oxidation of the central biphenylene unit under these conditions. The reductive segment of the cyclic voltammograms displayed a series of peaks. Quasi-reversible reduction processes are apparent with half-wave potentials of −1.10 and −1.32 V vs Ag/AgCl. Both processes correspond to three-electron steps, the former process being assigned to the reduction of the ethynylated ligands on the Ru-terpy units[29] and to reduction of one of the ligands associated with the Os-terpy center. It is well established that the ethynylene substituent renders the terpy ligand easier to reduce.[31] The process occurring at −1.32 V can be assigned to reduction of the capping terpyridine ligands on the Ru-terpy unit and of the remaining ligand resident on the Os-terpy center. The fact that this second reduction step occurs at a different potential to the first reduction of the Os-terpy group is most likely due to electrostatic factors.

Photophysical Properties. The absorption spectrum of **RBOBR** in acetonitrile at room temperature (Figure 4) displays the characteristic bands associated with bis(2,2′:6′,2″-terpyridine) complexes containing Os^{II} and Ru^{II} metal centers.[17] The broad absorption band centered around 500 nm is assigned to the metal-to-ligand charge transfer (MLCT) absorption bands for the Ru-terpy and Os-terpy units; they overlap such that individual bands cannot be resolved. There is also a low intensity tail stretching into the far-red region of the spectrum that can be assigned to the spin-forbidden MLCT transitions associated with the Os-terpy unit.[32] An expansion of this band clearly shows signs of vibrational splitting and locates the 0,0 transition

(29) Benniston, A. C.; Harriman, A.; Li, P.; Sams, C. A. *Phys. Chem. Chem. Phys.* **2004**, *6*, 875−877.
(30) Hissler, M.; Harriman, A.; El-ghayoury, A.; Ziessel, R. *Coord. Chem. Rev.* **1998**, *178*, 1251−1298.
(31) (a) Harriman, A.; Hissler, M.; Ziessel, R. *Phys. Chem. Chem. Phys.* **1999**, *1*, 4203−4211. (b) Hissler, M.; Harriman, A.; Khatyr, A.; Ziessel, R. *Chem.−Eur. J.* **1999**, *5*, 3366−3381.
(32) Decurtins, S.; Felix, F.; Ferguson, J.; Güdel, H. U.; Ludi, A. *J. Am. Chem. Soc.* **1980**, *102*, 4102−4106.

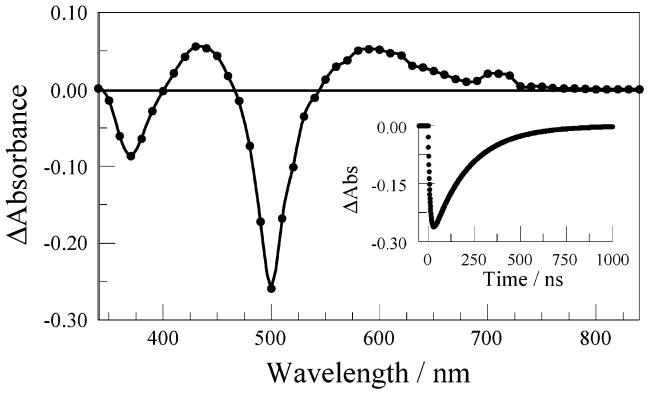

Figure 5. Transient differential absorption spectrum recorded at the end of a 4 ns laser pulse delivered at 532 nm for **RBOBR** in deoxygenated butyronitrile solution at room temperature. The insert shows a kinetic trace corresponding to recovery of the ground state recorded at 500 nm.

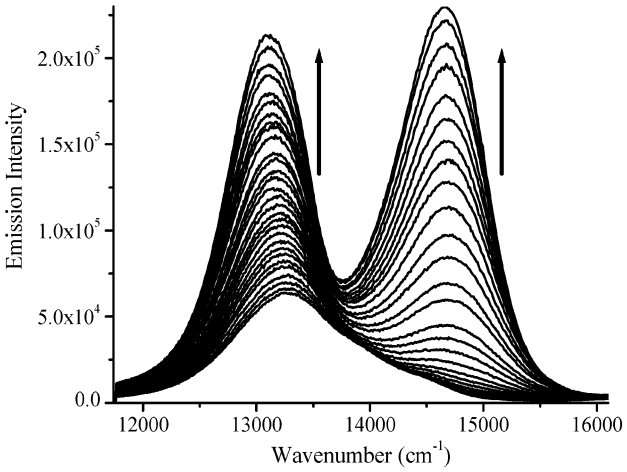

Figure 6. Effect of temperature on the luminescence spectra recorded for **RBOBR** in butyronitrile solution and with excitation at 500 nm.

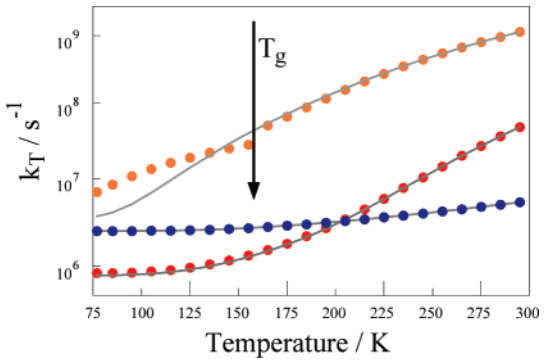

Figure 7. Effect of temperature on the rate constant for decay of the emitting triplet state isolated for the Os-terpy (blue) and Ru-terpy (orange) fragments present in **RBOBR** and for **RBR** (red) in butyronitrile solution. In each case, the solid line drawn through the data points is a nonlinear, least-squares fit to eq 1.

at 697 nm. Additional bands are seen in the near-UV region and assigned to ligand-centered transitions associated with both substituted and capping terpy ligands.[33] Excitation into the peak at 500 nm results in the appearance of a broad luminescence band centered around 750 nm (Figure 4). The emission profile and position are similar to those found for related Os-terpy derivatives.[34] There is no obvious indication of emission from the Ru-terpy unit, which is expected around 675 nm,[29] although this chromophore absorbs strongly at 500 nm. In fact, the excitation spectrum was found to give a good match with the absorption spectrum over the entire spectral region. This suggests that energy transfer from Ru-terpy to Os-terpy is efficient in the target compound. Close inspection of the high-energy part of the emission spectrum reveals a slight shoulder around 705 nm (Figure 4 and Supporting Information). This finding might be taken to suggest that the bridge emits under these conditions.[35] However, a similar luminescence profile is observed for the reference compound **7**, which does not possess the bridging portion of the molecule. Furthermore, we have found that the hot luminescence is, in fact, most likely from a second MLCT triplet state associated with the Os-terpy unit.[34]

The quantum yield (Φ_{LUM}) and lifetime (τ_{LUM}) measured for the total emission profile are 0.0031 ± 0.0005 and 195 ± 10 ns, respectively, following excitation at 650 nm where only the Os-terpy center absorbs. Again, these values compare well with results collected for the reference compound **7** and are essentially independent of excitation wavelength. The additional metal centers have little, if any, effect on the luminescence properties of the Os-terpy unit. Laser flash photolysis studies made with excitation at 532 nm show that the triplet excited state of the Os-terpy unit is present at the end of a 5 ns pulse (Figure 5). In deoxygenated acetonitrile, this latter species decays with a lifetime of 200 ± 10 ns. The characteristic transient absorption spectrum of the corresponding Ru-terpy unit[29] is not observed under these conditions. This finding indicates that the triplet lifetime of the Ru-terpy unit is less than ca. 5 ns, compared to a value of 25 ± 2 ns found for the reference compound **RBR**.[27a]

Both the yield and lifetime of the Os-terpy-based emission increase with decreasing temperature (Figure 6). A new luminescence band appears at low temperature, which by comparison with reference compound **RBR**, can be assigned to emission from the Ru-terpy-based terminals. The yield and lifetime of this new emission band also increase with decreasing temperature. Comparison with **RBR**, however, shows that emission from the Ru-terpy unit is always quenched with respect to the reference compound. This finding is consistent with intramolecular triplet energy transfer from the Ru-terpy-based terminals to the Os-terpy-based center.[2−11]

The temperature dependence found for the Os-terpy-based emission can be explained in terms of eq 1 (Figure 7).[36] Here, k_0 refers to the activationless rate constant for decay of the lowest-energy MLCT triplet state, and k_1 is the rate constant for decay of an upper MLCT triplet that is reached by passage over a small barrier, E_A. There is a metal-centered (MC) state lying at high energy that can be accessed by crossing a substantial barrier, E_B. The combined rate constant, k_2, for reaching the MC state is the sum of rate constants for promotion from both the MLCT triplets. The derived values are collected in Table 1 and remain comparable to data collected for related Os-terpy derivatives.[37] In particular, the k_1/k_0 ratio is in the range

(33) Khatyr, A.; Ziessel, R. *J. Org. Chem.* **2000**, *65*, 7814−7824.
(34) Benniston, A. C.; Harriman, A.; Li, P.; Sams, C. A. *J. Phys. Chem. A* In press.
(35) (a) Harriman, A.; Khatyr, A.; Ziessel, R. *Dalton Trans.* **2003**, 2061−2068. (b) Wang, Y. S.; Liu, S. X.; Pinto, M. R.; Dattelbaum, D. M.; Schoonover, J. R.; Schanze, K. S. *J. Phys. Chem. A* **2001**, *105*, 11118−11127. (c) Wang, B.; Wasielewski, M. R. *J. Am. Chem. Soc.* **1997**, *119*, 12−21.
(36) (a) Sacksteder, L. A.; Lee, M.; Demas, J. N.; DeGraff, B. A. *J. Am. Chem. Soc.* **1993**, *115*, 8230−8238. (b) Harrigan, R. W.; Hager, G. D.; Crosby, G. A. *Chem. Phys. Lett.* **1973**, *21*, 487−492.

Table 1. Parameters Derived from the Temperature Dependence Observed for the Deactivation of the Lowest-Energy MLCT Triplet State in Deoxygenated Acetonitrile Solution[a]

parameter	Os-terpy[b]	**RBR**	Ru-terpy[c]
$k_0/10^5\ s^{-1}$	24.2	8.3	32.6[e]
$k_1/10^8\ s^{-1}$	0.44	1.02	1.5[e], 33[f]
$k_2/10^{10}\ s^{-1}$	5.0	31.0	39.0[f]
E_A/kJ mol^{-1}	7.0	7.0	2.4[e], 6.0[f]
E_B/kJ mol^{-1}	30	22	15[f]
τ_T/ns[d]	200	25	0.95

[a] For both Os-terpy and **RBR**, the derived parameters refer to eq 1. [b] Refers to the Os-terpy center in **RBOBR**. [c] Refers to the Ru-terpy unit in **RBOBR**. [d] Measured at room temperature. [e] Refers to a glassy matrix. [f] Refers to butyronitrile solution.

found for other Os^{II} polypyridine complexes, while the barrier to reaching the MC state lies within the range expected for an Os^{II} polypyridine complex. The value found for k_0 is 2.4×10^6 s^{-1} and again is comparable to results found for related systems.[37] This is clear indication that the observed luminescence arises from the Os-terpy center.

$$k_T = \left(\frac{1}{\tau_{LUM}}\right) = \frac{k_0 + k_1 \exp\left(-\frac{E_A}{k_B T}\right) + k_2 \exp\left(-\frac{E_B}{k_B T}\right)}{1 + \exp\left(-\frac{E_A}{k_B T}\right) + \exp\left(-\frac{E_B}{k_B T}\right)} \quad (1)$$

The triplet lifetime recorded for the Ru-terpy reference compound **RBR** also follows eq 1 (Figure 7) but with the parameters listed in Table 1. The lowest-energy MLCT triplet state mixes with an upper MLCT triplet, reached by crossing a modest barrier set by E_A and a metal-centered state that is accessed by passage over a larger barrier, E_B. The activationless rate constant, found at low temperature, is smaller than that observed with the Os-terpy fragment because of the relative spin−orbit coupling constants.[38] Due to the increased perturbation caused by coupling to higher-energy states, the triplet lifetime of **RBR** at room temperature is considerably shorter than that of the Os-terpy fragment in **RBOBR** (Table 1). In contrast to this generic behavior, the triplet lifetime for the Ru-terpy fragment in **RBOBR**, this being measured by transient absorption spectroscopy, could not be fit to a single expression of the type described by eq 1. In a glassy matrix, the triplet decay rate constant, k_T, can be deconvoluted into activationless (k_0) and activated (k_1) rate constants, the latter being characterized by an activation energy (E_1) of 2.4 kJ mol^{-1} (Figure 7). This latter value is considerably smaller than the E_1 found for **RBR**, while the activationless rate constant, k_0, is some 4-fold higher (Table 1). In fluid solution, triplet decay is activated, and the observed rate constant follows eq 2 with the parameters collected in Table 1. The activation barrier, E_B, is much less than that normally associated with a Ru-terpy derivative reaching the MC state, while the activated rate constant, k_1, is inconsistent with either k_1 or k_2 found for **RBR**. The likelihood, therefore, is that a different quenching process is paramount in **RBOBR**. It is also important to note that whereas the triplet lifetime of **RBR** is 1.2 μs in a butyronitrile glass at 77 K, that of the Ru-terpy unit in **RBOBR** is only 165 ns.

$$k_T = \left(\frac{1}{\tau_{LUM}}\right) = k_1 \exp\left(-\frac{E_A}{RT}\right) + k_2 \exp\left(-\frac{E_B}{RT}\right) \quad (2)$$

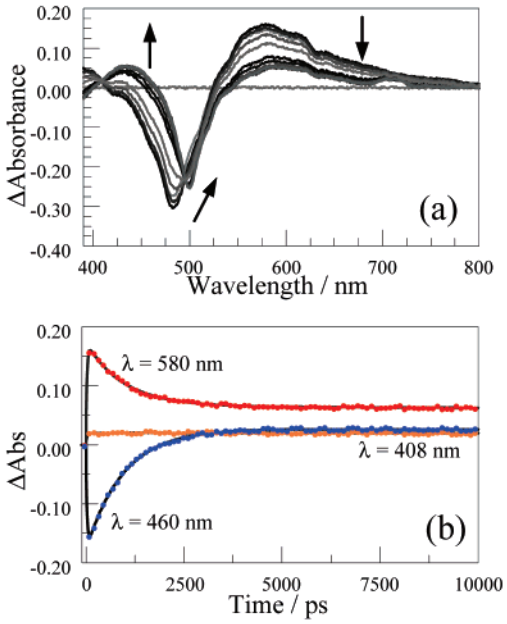

Figure 8. (a) Transient absorption spectra recorded at different times after excitation of **RBOBR** in deoxygenated butyronitrile at room temperature with a 25 ps laser pulse delivered at 480 nm. Delay times are: 0, 50, 100, 200, 400, 700, 1500, 2000, 3000, 5000, 7500, and 10 000 ps. (b) Kinetic traces recorded at 408, 460, and 580 nm.

Intramolecular Triplet Energy Transfer at Room Temperature. Comparison of the photophysical properties recorded for the Os-terpy and Ru-terpy centers present in **RBOBR** indicates quite clearly that emission from Os-terpy is unaffected by the presence of the second metal. In contrast, the yield and lifetime for emission localized on the Ru-terpy center are heavily quenched at all temperatures. Since intramolecular electron transfer is unlikely on thermodynamic grounds,[39] the most probable cause of emission quenching is triplet energy transfer for which there is a driving force of 17 kJ mol^{-1}. This situation is consistent with the observation that the corrected excitation spectrum is in good agreement with the absorption spectrum over the entire spectral range. Emission from the Ru-terpy terminal is too weak to be monitored accurately at room temperature, although comparison with **RBR** suggests that the extent of quenching is ca. 95%. Transient absorption spectroscopy, made following laser excitation at 480 nm with a 25 ps pulse, showed that the triplet lifetime of the Ru-terpy unit was 0.95 ± 0.05 ns (Figure 8). This can be compared to a triplet lifetime of 25.0 ± 1.5 ns measured for **RBR** under identical conditions. Thus, the apparent rate constant for triplet energy transfer (k_{TT}) in **RBOBR** at room temperature is $(1.05 \pm 0.05) \times 10^9\ s^{-1}$, while the efficiency of the energy-transfer step calculated from the kinetic measurements is ca. 95%. Time-resolved emission studies confirmed that about 70% of the emission due to the Os-terpy center grows in with a first-order rate constant of $(1.0 \pm 0.1) \times 10^9\ s^{-1}$ (Figure 9). The overall system, therefore, appears to be consistent with efficient intramolecular triplet energy transfer to the central Os-terpy unit,

(37) Lumpkin, R. S.; Kober, E. M.; Worl, L. A.; Murtaza, Z.; Meyer, T. J. *J. Phys. Chem.* **1990**, *94*, 239−243.
(38) Spin−orbit coupling constants of 3381 and 1042 cm^{-1} have been reported for osmium and ruthenium, respectively: Murov, S. L.; Carmichael, I.; Hug, G. L. *Handbook of Photochemistry*; Marcel Dekker: New York, 1993.
(39) According to the measured reduction potentials and triplet energy, light-induced electron transfer to ($\Delta G° = +0.62$ eV) or from ($\Delta G° = +0.30$ eV) the triplet state of the Ru-terpy unit is unlikely to compete with nonradiative decay of the excited state.

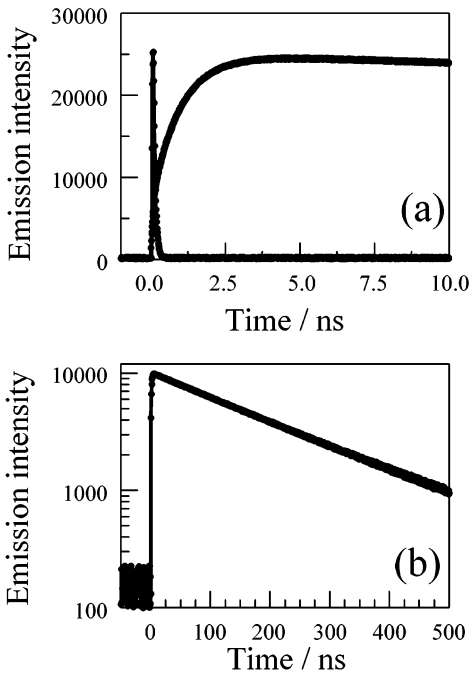

Figure 9. Time-resolved luminescence decay profiles recorded at 750 nm for **RBOBR** in deoxygenated acetonitrile at room temperature. (a) Decay curve recorded on a short time scale following laser excitation with 50 ps temporal resolution. The sharp curve is the instrument response function. (b) Decay curve recorded on a longer time scale showing decay of the Os-terpy triplet.

despite the 25 Å separation. There are many related systems in the literature that demonstrate triplet−triplet energy transfer in fluid solution.[2−11]

Triplet Energy Transfer in a Frozen Glass. Similar measurements were made as a function of temperature. First, experiments were made in a butyronitrile glass using excitation at 480 nm with a 4 ns laser pulse. Emission from the Ru-terpy unit was isolated with a high radiance monochromator and the lifetime recorded at different temperatures. At all temperatures below the glass melting point (T_g = 161 K), the measured lifetime (τ_{RU}) was notably shorter than that recorded for **RBR** (τ_{REF}) under identical conditions (see Supporting Information). Confirmation that quenching was due to intramolecular triplet energy transfer was obtained by the fact that a substantial (i.e., >60%) fraction of the emission associated with the Os-terpy grows in after the excitation pulse and on the same time scale as decay of the triplet localized on the Ru-terpy unit. The rate constant for triplet energy transfer (k_{TT}) was determined as the difference between the two triplet lifetimes for the Ru-terpy emission.

$$k_{TT} = \frac{1}{\tau_{RU}} - \frac{1}{\tau_{REF}} \tag{3}$$

The derived rate constant shows a weak dependence on temperature throughout the glassy region (Figure 10). In fact, there is a good fit to a modified Arrhenius-type expression comprising both activated (k_D) and activationless (k_F) components.

$$k_{TT} = k_F + k_D e^{-\Delta G/RT} \tag{4}$$

Extrapolation of the data gives values for k_D and k_F of (1.4 ± 0.2) × 10^8 and (2.2 ± 0.2) × 10^6 s^{-1}, respectively, while the apparent activation energy ($\Delta G^{\ddagger}$) is 2.3 ± 0.2 kJ mol^{-1}. The value for the activationless rate constant is remarkably similar to the calculated rate constant for Förster-type energy transfer (k_{FOR} = 3.2 × 10^6 s^{-1}). This latter value was computed on the basis of spectroscopic properties measured for the relevant chromophores present in **RBOBR** and by using the photophysical properties recorded for **RBR** in a low-temperature glass.[27a] On the basis that k_F refers to Förster-type energy transfer, it is reasonable to suppose that k_D corresponds to Dexter-type electron exchange since this process is expected to be weakly activated.[40]

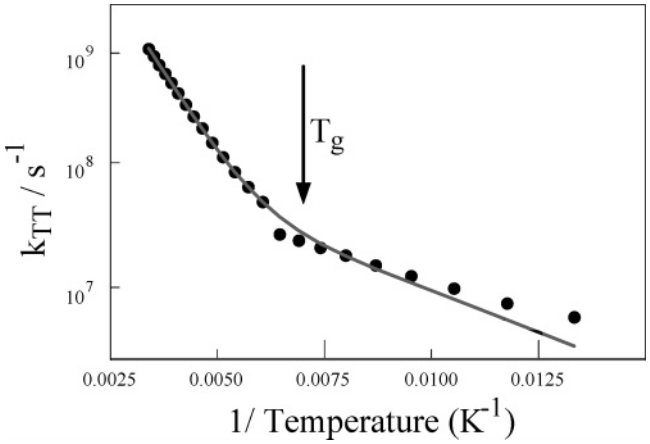

Figure 10. Effect of temperature on the rate constant for triplet−triplet energy transfer measured for **RBOBR** in butyronitrile. T_g indicates the glass transition temperature, while the solid line drawn through the data points corresponds to a nonlinear, least-squares fit to eq 9 with the parameters listed in the text.

Table 2. Parameters Extracted from Spectral Curve Fitting of the Emission Spectrum Recorded for **RBOBR** in a Butyronitrile Glass at 140 K and Used To Calculate the Franck−Condon Factor

property	Os-terpy[a]	Ru-terpy[b]
E_T/cm^{-1} [c]	13475	14905
λ_T/cm^{-1} [d]	220	450
$h\omega_M$/cm^{-1} [e]	1370	1400
S_M[f]	0.38	0.50

[a] Refers to the Os-terpy center in **RBOBR**. [b] Refers to the Ru-terpy terminal in **RBOBR**. [c] Triplet energy of the respective luminescent center. [d] Reorganization energy accompanying deactivation of the lowest-energy MLCT triplet state. [e] Medium-frequency vibrational mode coupled to nonradiative decay of the triplet state. [f] Huang−Rhys factor for the medium-frequency vibrational mode.

The activation energy for triplet energy transfer ($\Delta G^{\ddagger}_{FC}$) can be calculated from a Franck−Condon analysis[41] of the emission spectra according to eqs 5−8. Here, V_{DA} is the matrix element for electron exchange; λ_{TT} is the reorganization energy accompanying triplet energy transfer, while the terms S_A and S_D refer to the electron-vibrational coupling constants for acceptor and donor, respectively. The energy gap between triplet states localized on donor and acceptor is designated as ΔE_{TT}, while $h\omega_D$ and $h\omega_A$ refer to medium-frequency vibrational modes coupled to the respective MLCT transitions in donor and acceptor species. The indices *m* and *n* are vibrational quantum numbers for donor and acceptor species. Each of these parameters can be determined by fitting low-temperature emission spectra for the donor and acceptor, and a compilation of the derived data is given in Table 2. The value calculated for $\Delta G^{\ddagger}_{FC}$ in this way is 2.6 kJ mol^{-1}, which places electron

exchange slightly in the Marcus inverted region ($\Delta E_{TT} \approx -2\lambda_{TT}$).

$$k_D = (k_{TT} - k_F) \quad (5)$$

$$k_D = \frac{2\pi}{\hbar}|V_{DA}|^2 FC \quad (6)$$

$$FC = \left(\frac{1}{\sqrt{4\pi\lambda_{TT}k_BT}}\right)\sum_{m=0}^{\infty}\sum_{n=0}^{\infty} e^{-S_D}e^{-S_A}\left(\frac{S_D^m}{m!}\right)\left(\frac{S_A^n}{n!}\right)e^{-\Delta G_{FC}^{\ddagger}/k_BT} \quad (7)$$

$$\Delta G_{FC}^{\ddagger} = \left(\frac{(\Delta E_{TT} + \lambda_{TT} + m\hbar\omega_D + n\hbar\omega_A)^2}{4\lambda_{TT}}\right) \quad (8)$$

The calculated activation energy for electron exchange in a glassy matrix can now be compared to the experimental value of 2.3 ± 0.2 kJ mol^{-1}. The two values are remarkably close and appear to be entirely consistent with the notion that energy transfer in a frozen glass is due to a combination of Förster- and Dexter-type mechanisms, with the latter predominating at higher temperature. The excellent agreement between calculated and experimental activation energies provides strong support for the idea that electron exchange involves long-range superexchange interactions between the reactants.[42] There is no indication for the bridge acting as a "real" intermediate in this process. Using the computed Franck−Condon factor (FC = 4.8 × 10^{-5} cm) together with the derived k_D (6.0 × 10^6 s^{-1}) value at 77 K indicates that, under these conditions, V_{DA} is 0.32 cm^{-1}. This seems to be a reasonable value for long-range triplet−triplet energy transfer in view of literature reports for somewhat related systems at room temperature.[7] The limiting value for k_D (1.4 × 10^8 s^{-1}) seems to be rather slow when compared to other systems; for example, electron exchange across two phenylene rings occurs with a rate constant of >3 × 10^{10} s^{-1} at room temperature.

Triplet Energy Transfer in Fluid Solution. Above the glass transition temperature, k_{TT} advances more steeply with increasing temperature (Figure 10). In the high-temperature region, the observed rate constant for triplet energy transfer fits well to eq 9. The weakly activated component (k_D = 1.5 × 10^8 s^{-1}; $\Delta G^{\ddagger}$ = 2.3 kJ mol^{-1}) agrees with that attributed to electron exchange, but there is an additional component characterized by a rate constant (k_{ACT}) of (1.7 ± 0.2) × 10^{11} s^{-1} and an activation energy (E_{ACT}) of 12.5 ± 1.0 kJ mol^{-1}. It is important to note that the more strongly activated process does not contribute to the overall behavior in a glassy matrix. This new kinetic component, therefore, is a feature of the fluid solution. It is unlikely that Förster-type energy transfer makes a serious contribution to the global process under these conditions since the calculated k_{FOR} value remains at ca. 3 × 10^6 s^{-1}. Likewise, the Franck−Condon factor[41] (FC = 5.1 × 10^{-5} cm) is similar to that found for a glassy matrix. As such, there is no obvious reason, at least in electronic terms, for either the increased rate or the higher activation energy found in fluid solution. Indeed, using the measured k_{TT} at room temperature in conjunction with the calculated Franck−Condon factor requires that the electronic coupling matrix element for electron exchange (V_{DA}) increases to 4.2 cm^{-1}. This is a 13-fold increase relative to the value determined for electron exchange in a glassy matrix.

$$k_{TT} = k_D e^{-\Delta G/k_BT} + k_{ACT}\, e^{-E_{ACT}/k_BT} \quad (9)$$

It is recognized that the rate of through-bond electron exchange should be sensitive to the stereochemistry of the bridging unit.[43] Although the torsion angle around the central biphenylene unit is 37° for the lowest-energy conformer, molecular dynamics simulations indicate that there is considerable internal flexibility about the connecting bond (Figure 3). These studies show that the torsion angle for either atropisomer can vary from 54 to 20° and, as such, it seems reasonable to suppose that the rate of through-bond electron exchange is dependent on the actual geometry of the bridge. Other researchers have reached similar conclusions for both electron transfer[44] and electron exchange.[43,45] On this basis, we can safely assign the limiting k_D (1.4 × 10^8 s^{-1}) value found in the low-temperature region to electron exchange through a torsion angle of 37°.

In the high-temperature limit, the maximum rate constant for electron exchange in **RBOBR**, taken to correspond to k_{ACT} in eq 9, has a value of 1.7 × 10^{11} s^{-1}. It is tempting to assign this rate to electron exchange across the most favorable orientation of the bridge; presumably, this refers to a coplanar arrangement of the biphenylene unit although the tethering strap does not permit adoption of this geometry. As such, V_{DA} for electron exchange across the most favorable geometry would need to increase to 53 cm^{-1}. This seems to be an unreasonably high value for triplet energy transfer across 25 Å.[7] Furthermore, the variation in V_{DA} as the angle changes seems to be unrealistically high based on earlier measurements made for hole transfer between the metal centers in related binuclear Ru^{II} complexes.[46]

The indications are that the long-range superexchange mechanism does not hold for the high-temperature region; the derived $\Delta G^{\ddagger}$, k_{TT}, and V_{DA} values are too high to be consistent with eqs 5−8. While it seems plausible that internal rotation around the connecting biphenylene ring will contribute to variations in k_{TT},[47] the observed experimental results imply that a different mechanism operates at high temperature. Given the high V_{DA}, it is likely that this additional mechanism involves short-range interactions associated with the bridging unit. There is no indication for low-lying π,π^* triplet states localized on the bridge, but molecular orbital studies made with the corresponding zinc(II) complex show that there is an intramolecular charge-transfer (CT) state situated at relatively low energy. This CT

(40) Long-range triplet energy transfer can be equated to simultaneous transfer of an electron and a positive hole for which the activation energy can be derived from classical Marcus theory. Since the driving force and the reorganization energy are of comparable magnitude, it follows that the reaction should be weakly activated.

(41) Murtaza, Z.; Graff, D. K.; Zipp, A. P.; Worl, L. A.; Jones, W. E.; Bates, W. D.; Meyer, T. J. *J. Phys. Chem.* **1994**, *98*, 10504−10513.
(42) (a) Liang, N.; Miller, J. R.; Closs, G. L. *J. Am. Chem. Soc.* **1990**, *112*, 5353−5354. (b) Liang, N.; Miller, J. R.; Closs, G. L. *J. Am. Chem. Soc.* **1989**, *111*, 8740−8741.
(43) Closs, G. L.; Piotrowiak, P.; MacInnis, J. M.; Fleming, G. R. *J. Am. Chem. Soc.* **1988**, *110*, 2652−2653.
(44) Closs, G. L.; Calcaterra, L. T.; Green, N. J.; Penfield, K. W.; Miller, J. R. *J. Phys. Chem.* **1986**, *90*, 3673−3683.
(45) (a) Kroon, J.; Oliver, A. M.; Paddon-Row, M. N.; Verhoeven, J. W. *J. Am. Chem. Soc.* **1990**, *112*, 4868−4673. (b) Oevering, H.; Verhoeven, J. W.; Paddon-Row, M. N.; Cotsaris, E.; Hush, N. S. *Chem. Phys. Lett.* **1988**, *150*, 179−180.
(46) Benniston, A. C.; Harriman, A.; Li, P.; Sams, C. A.; Ward, M. D. *J. Am. Chem. Soc.* **2004**, *126*, 13630−13631.
(47) (a) Helms, A.; Heiler, D.; McLendon, G. *J. Am. Chem. Soc.* **1992**, *114*, 6227−6238. (b) Helms, A.; Heiler, D.; McLendon, G. *J. Am. Chem. Soc.* **1991**, *113*, 4325−4327.

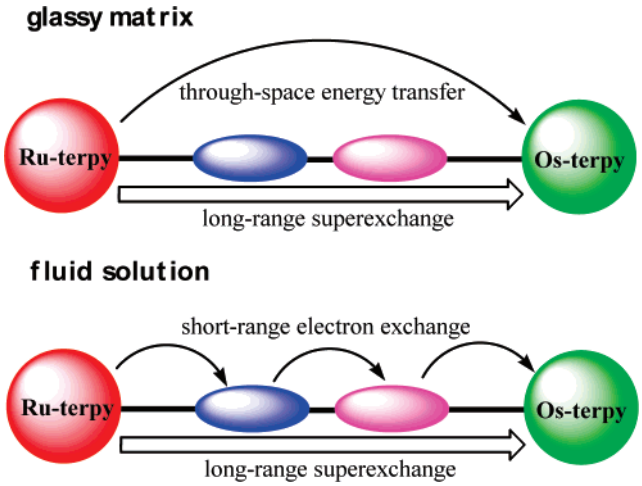

Figure 11. Pictorial representation of triplet energy transfer occurring in fluid solution and in a glassy matrix.

state is formed by electron donation from the alkoxybenzene donor to the coordinated terpy ligand bearing the ethynylene group. The energy of this state depends on solvent polarity and will be inaccessibly high in a glassy matrix.[48] However, in fluid solution, the energy of the CT state approaches that of the Ru-terpy MLCT state, without falling below it, such that it could be populated from the Ru-terpy-based donor at ambient temperature (Figure 11). The measured activation energy of 12.5 kJ mol^{-1}, therefore, can be taken to represent the barrier for access to this bridge-localized CT state.

It should be noted that there is strong experimental support for the involvement of such CT states in the triplet manifold of platinum terpyridine complexes substituted with aryl groups.[49] The photophysical properties of these latter complexes are set by the interplay between ligand-localized π,π^* triplets and CT states. The significance of the CT interactions increases as the substituents become more electron donating. Although direct spectroscopic evidence for the population of intraligand CT states in **RBOBR** is lacking, it seems highly likely that such states contribute to the energy-transfer sequence in polar solution.

Intramolecular triplet energy transfer in the high-temperature limit can now be described in terms of a series of short-range steps (Figure 11). Thus, in competition with long-range, superexchange-mediated energy transfer to the Os-terpy acceptor, the lowest-energy MLCT triplet localized on Ru-terpy transfers energy to the adjacent CT triplet state. The proximity of these reactants should favor a high V_{DA}, but there is likely to be a substantial reorganization energy for this step because of the difference in geometries. The resultant CT state can transfer triplet energy to the corresponding CT state associated with the Os-terpy.[50] This step involves crossing the biphenylene unit, but the two triplets are likely to be almost isoenergetic. The latter CT state can transfer energy to the Os-terpy MLCT triplet state by way of a strongly exoergonic reaction. Except

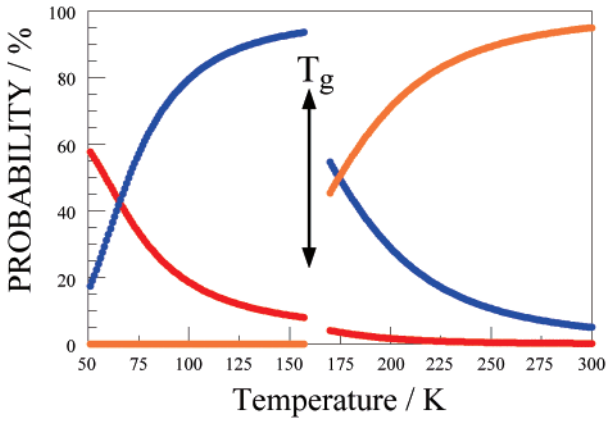

Figure 12. Relative contribution of each of the three mechanisms toward triplet energy transfer in **RBOBR** as a function of temperature: Förster-type energy transfer (red), long-range superexchange (blue), and short-range charge hopping (orange).

for the final step, each energy-transfer process should be reversible. The overall reaction will be driven toward net energy transfer, however, since the Os-terpy triplet acts as an energy sink. In order for the process to remain efficient, it is necessary to propose that direct deactivation of the CT triplet to the ground state is relatively slow. This seems a reasonable assumption since direct charge recombination will lie deep within the Marcus inverted region.[51] It will also explain why the intermediary CT state does not perturb the photophysical properties of the reference compound **RBR**. On this basis, k_{ACT} is set primarily by the rate of population of the CT triplet.

Concluding Remarks

Three separate mechanisms have been identified for intramolecular triplet energy transfer in **RBOBR**. At very low temperature in a glassy matrix, the limiting rate of energy transfer is set by Förster-type dipole−dipole interactions. This step is sufficiently fast to ensure that triplet energy transfer occurs with a probability of ca. 80%.[52] At higher temperature in the glass, Dexter-type electron exchange takes place via a weakly activated process. This long-range, superexchange-mediated mechanism dominates from 77 K to the glass transition temperature. It is believed that this step involves electron exchange across the bridging biphenylene unit which is held in the lowest-energy conformation. A strongly activated process takes over in fluid solution and pushes the probability of energy transfer up to around 95%. This latter step involves transient population of a CT state localized on the bridge, followed by energy migration and trapping by the Os-terpy-based acceptor. The involvement of an intermediate CT state that does not decay directly to the ground state is favored by a polar solvent and ambient temperature. Thus, the significance of any given mechanism depends on temperature (Figure 12).

(48) (a) Harriman, A.; Heitz, V.; Ebersole, M.; van Willigen, H. *J. Phys. Chem.* **1994**, *98*, 4982−4989. (b) Wasielewski, M. R.; Johnson, D. G.; Svec, W. A.; Kersey, K. M.; Minsek, D. W. *J. Am. Chem. Soc.* **1988**, *110*, 7219−7221. (c) Heitele, H.; Finckh, P.; Weeren, S.; Pollinger, F.; Michel-Beyerle, M. E. *J. Phys. Chem.* **1989**, *93*, 5173−5179.

(49) (a) Michalec, J. F.; Bejune, S. A.; Cuttell, D. G.; Summerton, G. C.; Gertenbach, J. A.; Field, J. S.; Haines, R. J.; McMillin, D. R. *Inorg. Chem.* **2001**, *40*, 2193−2200. (b) Michalec, J. F.; Bejune, S. A.; McMillin, D. R. *Inorg. Chem.* **2000**, *39*, 2708−2709.

(50) It seems likely that restricted rotation around the central biphenylene group will prevent this unit from acting as the electron donor. Instead, each phenylene ring is expected to donate charge to the nearest terpyridine ligand. Since the reduction potentials for Os-terpy and Ru-terpy are closely comparable, the latter situation would give rise to two CT states of similar energy and geometry. Energy migration between these triplets should be fast.

(51) (a) Amini, A.; Harriman, A. *J. Phys. Chem. A* **2004**, *108*, 1242−1249. (b) Brun, A. M.; Harriman, A.; Tsuboi, Y.; Okada, T.; Mataga, N. *J. Chem. Soc., Faraday Trans.* **1995**, *91*, 4047−4057. (c) Wasielewski, M. R.; Minsek, D. W.; Niemczyk, A.; Svec, W. A.; Yang, N. C. *J. Am. Chem. Soc.* **1990**, *112*, 2823−2824.

(52) Probability calculated according to $P_T = k_{TT}\tau_{LUM}$, with both rate constant and lifetime being measured at a given temperature.

Two important realizations stem from the above discussion. First, the involvement of an intermediary CT triplet could have important implications for the design of systems capable of very long range energy transfer.[53] This is a key objective for the future evolution of effective molecular-scale photonic devices. Second, electron exchange in a glassy matrix appears to operate by way of a long-range superexchange mechanism. This involves simultaneous electron and hole transfer through the bridging biphenylene unit and, as such, the rate should be a function of the torsion angle at the center. Our work refers to a torsion angle of 37°, but this can be varied systematically by increasing the length of the tethering strap.[14a,b] Such studies are in progress.

(53) This possibility stems from the likelihood that fast energy migration could occur between isoenergetic CT states, followed by trapping at a low-energy acceptor.

Acknowledgment. This work was supported by the EPSRC (GR/R23305/01 and GR/S00088/01) and by the University of Newcastle. We are greatly indebted to Johnson Matthay Ltd. for the loan of precious metal salts. We also thank the EPSRC-funded Mass Spectrometry Service at Swansea for recording MALDI and electrospray mass spectra.

Supporting Information Available: Luminescence spectra recorded for Os-terpy and Os-acet in butyronitrile solution, showing the contribution made by the "hot" band, and a table giving the triplet lifetimes recorded for the various excited states at different temperature. This material is available free of charge via the Internet at http://pubs.acs.org.

JA044097R